SLAC–PUB–4952
May 1989
T/E

Observation of $D_s^+ \rightarrow \bar{K}^0 K^+$ and $D_s^+ \rightarrow \bar{K}^{*0} K^+$ and an Upper Limit on $D_s^+ \rightarrow K^0 \pi^+$ †

J. Adler, Z. Bai, J.J. Becker, G.T. Blaylock, T. Bolton, J.-C. Brient, J.S. Brown, K.O. Bunnell, M. Burchell, T.H. Burnett, R.E. Cassell, D. Coffman, V. Cook, D.H. Coward, F. DeJongh, D.E. Dorfan, J. Drinkard, G.P. Dubois, G. Eigen, K.F. Einsweiler, B.I. Eisenstein, T. Freese, C. Gatto, G. Gladding, C. Grab, R.P. Hamilton,‡ J. Hauser, C.A. Heusch, D.G. Hitlin, J.M. Izen, P.C. Kim, L. Köpke, J. Labs, A. Li, W.S. Lockman, U. Mallik, C.G. Matthews, A.I. Mincer, R. Mir, P.M. Mockett, B. Nemati, A. Odian, L. Parrish, R. Partridge, D. Pitman, S.A. Plaetzer, J.D. Richman, M. Roco, H.F.W. Sadrozinski, M. Scarlatella, T.L. Schalk, R.H. Schindler, A. Seiden, C. Simopoulos, A.L. Spadafora, I.E. Stockdale, W. Stockhausen, W. Toki, B. Tripsas, F. Villa, M.Z. Wang, S. Wasserbaech, A. Wattenberg, A.J. Weinstein, S. Weseler, H.J. Willutzki, D. Wisinski, W.J. Wisniewski, R. Xu, Y. Zhu

The Mark III Collaboration

California Institute of Technology, Pasadena, CA 91125
University of California at Santa Cruz, Santa Cruz, CA 95064
University of Illinois at Urbana-Champaign, Urbana, IL 61801
University of Iowa, Iowa City, IA 52242
Stanford Linear Accelerator Center, Stanford, CA 94309
University of Washington, Seattle, WA 98195

Abstract

We report the first observation of the decay $D_s^+ \rightarrow \bar{K}^0 K^+$ and a new measurement of the decay $D_s^+ \rightarrow \bar{K}^*(892)^0 K^+$. The data were collected at $\sqrt{s} = 4.14$ GeV with the Mark III detector at SPEAR. We obtain the relative branching fractions $B(D_s^+ \rightarrow \bar{K}^0 K^+)/B(D_s^+ \rightarrow \phi\pi^+) = 0.92 \pm 0.32 \pm 0.20$ and $B(D_s^+ \rightarrow \bar{K}^{*0} K^+)/B(D_s^+ \rightarrow \phi\pi^+) = 0.84 \pm 0.30 \pm 0.22$, using our new determination of $\sigma B(D_s^+ \rightarrow \phi\pi^+)$. A search for the Cabibbo-suppressed decay $D_s^+ \rightarrow K^0\pi^+$ yields a limit $B(D_s^+ \rightarrow K^0\pi^+)/B(D_s^+ \rightarrow \phi\pi^+) < 0.21$ at the 90% confidence level.

Submitted to *Physical Review Letters*

† This work was supported in part by the U. S. Department of Energy, under contracts DE-AC03-76SF00515, DE-AC02-76ER01195, DE-AC02-87ER40318, DE-AC03-81ER40050, DE-AM03-76SF0034, and by the National Science Foundation.

‡ Deceased.

The weak hadronic decays of D^0 and D^+ mesons have been studied in detail by numerous experiments. Most of these results are understood within the framework of QCD-corrected models,[1] which predict an enhancement of the non-leptonic partial widths of both the D^0 and D^+ over the naive spectator model values. No unambiguous evidence for significant exclusive non-spectator processes (W-exchange or W-annihilation) has yet been observed in D^0, D^+, or D_s^+ decays.[2–5] The difference in the D^0 and D^+ total non-leptonic transition rates[6,7] is thought to arise largely from the presence of interference in D^+ decays.[8,9] The effects of non-spectator diagrams may be understood from further measurements of exclusive charm decay modes. We present herein the first evidence for the decay[10] $D_s^+ \to \bar{K}^0 K^+$, a new measurement of the decay $D_s^+ \to \bar{K}^*(892)^0 K^+$, and an upper limit for the decay $D_s^+ \to K^0 \pi^+$. These results allow further quantitative tests of theoretical predictions of weak charm decays to exclusive hadronic final states.

The data sample, a total of $6.30 \pm 0.46\,\mathrm{pb}^{-1}$, was collected at $\sqrt{s} = 4.14\,\mathrm{GeV}$ with the Mark III detector[11] at the e^+e^- storage ring SPEAR. In this analysis, data from the main drift chamber, the time-of-flight system (TOF), and the dE/dx system are used. At $\sqrt{s} = 4.14\,\mathrm{GeV}$, D_s^+ mesons are produced predominantly in the reactions[12] (a) $e^+e^- \to D_s^\pm D_s^{*\mp}$ and (b) $D_s^{*\mp} \to \gamma D_s^\mp$. The $D_s^\pm$ produced by reaction (a) is referred to as *primary*, while that produced by reaction (b) is referred to as *secondary*. The primary $D_s^\pm$ is produced with a fixed momentum of $0.35\,\mathrm{GeV}/c$, while the secondary $D_s^\mp$ is produced with momentum between 0.18 and $0.47\,\mathrm{GeV}/c$. These production kinematics are exploited both to reduce backgrounds and to improve the D_s^+ mass resolution.

The search for $D_s^+ \to \bar{K}^0 K^+$ is made in the $K_S^0 K^+ \to \pi^+\pi^- K^+$ final state.

Kaon and pion candidates are selected using particle identification information from TOF and dE/dx.[13] Candidate K^0_S's are formed from all $\pi^+\pi^-$ combinations in which the reconstructed K^0_S decay vertex is displaced from the average beam position by a distance $\delta > 3\,\mathrm{mm}$ normal to the beam axis. This requirement significantly reduces combinatoric background (Figure 1), while rejecting only 9% of the $K^0_S \to \pi^+\pi^-$ decays from $D_s^+ \to \bar{K}^0 K^+$.

Accepted $\pi^+\pi^- K^+$ combinations are kinematically fitted to the hypothesis $e^+e^- \to K^0_S K^+ D_s^{*-}$, where the D_s^{*-} is not reconstructed.[14] Candidates with fit χ^2 confidence level CL $> 10\%$ are retained, resulting in the $K^0_S K^+$ mass distribution in Fig. 2(a). An enhancement is observed at the D_s^+ mass. The fit hypothesis is correct only for decays of primary D_s^+'s, which are reconstructed with a mass resolution of $\sim 5\,\mathrm{MeV}/c^2$. The fit also retains secondary decays with 2/3 of the efficiency for primary decays. These secondary D_s^+ candidates, however, have a broader mass distribution which extends $\pm 50\,\mathrm{MeV}/c^2$ about the D_s^+ mass.

To verify that the peak at $1.97\,\mathrm{GeV}/c^2$ arises from $D_s^+ \to \bar{K}^0 K^+$, both the recoil mass constraint and the δ cut are varied. No signal is observed when the imposed recoil mass constraint is placed outside the D_s^* mass region. The observed reduction of the signal when the minimum δ requirement is raised to 5 mm is consistent with Monte Carlo predictions.

The background contribution arising from D^0 and D^+ decays is predicted with a Monte Carlo simulation [dashed histogram in Fig. 2(b)]. At $\sqrt{s} = 4.14\,\mathrm{GeV}$, D mesons are copiously produced in the final states $D^*\bar{D}^*$, $D^*\bar{D}$, and $D\bar{D}$, with production cross sections and decay branching fractions which are well measured in our own data at 3.77 GeV and at 4.14 GeV.[2,6,15,16] No enhancement in the D_s^+ region is predicted to arise from D meson decays or from other D_s^+ decay modes.

The number of observed $D_s^+ \to K_S^0 K^+$ decays, 23.3 ± 5.9, is determined by fitting the mass spectrum in Fig. 2(a). The shape of the background is taken from the solid histogram in Fig. 2(b), which shows the sum of the predicted contributions from non-charm continuum events[17] and D decays. The total of these contributions is consistent with the observed number of background entries. Nevertheless, the normalization of the background is allowed to vary in the fit. The shapes and relative amounts of the primary and secondary signal contributions are also obtained by Monte Carlo calculation. We assume $B(D_s^{*+} \to \gamma D_s^+) = 100\%$. The average detection efficiency, including $B(\bar{K}^0 \to \pi^+\pi^-)$, is 7.8%. This yields the cross-section times branching fraction $\sigma B(D_s^+ \to \bar{K}^0 K^+) = 24 \pm 6 \pm 5\,\mathrm{pb}$, where $\sigma \equiv \sigma(e^+e^- \to D_s^+ D_s^{*-} + D_s^- D_s^{*+})$. The estimate of the systematic error accounts for the uncertainty in the background shape (13%), the detection efficiency (16%), the integrated luminosity (7%), and the mass of the D_s^{*-} (1%).

To search for the Cabibbo-suppressed decay $D_s^+ \to K^0\pi^+$, a similar procedure is followed.[18] The resulting $K_S^0\pi^+$ mass spectrum appears in Fig. 3(a). Monte Carlo signal and background shapes are determined as in the $D_s^+ \to \bar{K}^0 K^+$ analysis. The predicted number of D and continuum entries agrees with the observed spectrum [Fig. 3(b)]. A 90% CL upper limit of 3.8 signal events is obtained by integrating the likelihood function. Allowing for efficiency (9.5%) and increasing the limit by the systematic uncertainty (18%) yields $\sigma B(D_s^+ \to K^0\pi^+) < 3.7\,\mathrm{pb}$ (90% CL).

The $D_s^+ \to \bar{K}^*(892)^0 K^+$ decay is studied in the $K^+K^-\pi^+$ final state. The inclusive $K^-\pi^+$ mass spectrum is shown in Fig. 4. A $\bar{K}^{*0}$ signal is observed with the expected mass and width. A one-constraint kinematic fit to the hypothesis $e^+e^- \to K^+K^-\pi^+D_s^{*-}$ is performed for each $K^+K^-\pi^+$ combination. The $\bar{K}^{*0}K^+$ mode is selected by requiring the fitted $K^-\pi^+$ mass to be within $75\,\mathrm{MeV}/c^2$ of the nominal $\bar{K}^{*0}$ mass. For the reaction $D_s^+ \to \bar{K}^{*0}K^+$, $\bar{K}^{*0} \to K^-\pi^+$, the polar angle θ_π of the π^+ in the $\bar{K}^{*0}$ helicity frame is expected to have a $\cos^2\theta_\pi$ distribution. The requirement $|\cos\theta_\pi| > 0.3$ is imposed to improve the signal-to-background ratio. The resulting $\bar{K}^{*0}K^+$ mass distribution [Fig. 5(a)] shows a D_s^+ signal. The validity of the $D_s^+ \to \bar{K}^{*0}K^+$ signal is checked by examining $\bar{K}^{*0}$ sidebands and by varying the recoil mass constraint. No peak is observed at the D_s^+ mass in either case.

The mass spectrum in Fig. 5(a) is fitted by the procedure used in the $\bar{K}^0K^+$ analysis. The predicted background contribution from D decays and non-charm continuum events [Fig. 5(b)] is again consistent with the observed total background. The signal contains 23.8 ± 6.3 entries. A subtraction is made for two sources of background which produce enhancements at or near the D_s^+ mass: $D^+ \to \bar{K}^{*0}\pi^+$ (0.8 ± 0.6 events[15]) and non-resonant $D_s^+ \to K^+K^-\pi^+$ (1.8 ± 0.8 events[19]). The decay $D_s^+ \to \phi\pi^+$ is excluded by the $\bar{K}^{*0}$ requirement on the $K^-\pi^+$ mass. The detection efficiency for $D_s^+ \to \bar{K}^{*0}K^+$, including $B(\bar{K}^{*0} \to K^-\pi^+)$, is 7.8%, yielding $\sigma B(D_s^+ \to \bar{K}^{*0}K^+) = 22 \pm 6 \pm 6\,\mathrm{pb}$. The estimate of the systematic error accounts for the uncertainty in the shape of the smooth background (21%), the Monte Carlo efficiency (14%), the integrated luminosity (7%), and the subtraction of background from the signal peak (5%).

To obtain more precise measurements of D_s^+ decay modes relative to $\phi\pi^+$, we have improved our determination[12] of $\sigma B(D_s^+ \to \phi\pi^+)$ by using the same kinematic fitting technique. The systematic uncertainty on the reconstruction efficiency has been reduced to 14% by further study of D decays in the same data set. The result is $\sigma B(D_s^+ \to \phi\pi^+) = 26 \pm 6 \pm 5\,\mathrm{pb}$. Our measured relative branching fractions are given in Table I. The $\bar{K}^{*0}K^+$ result is consistent with previous measurements.[19–22]

The predictions of a factorization calculation[9] (Model 1), a QCD sum rule analysis[23] (Model 2), and a model with final state interactions[24] (Model 3) are compared with the observed relative branching fractions in Table I. The decays $D_s^+ \to \bar{K}^0K^+$, $\bar{K}^{*0}K^+$, and $K^0\pi^+$ may proceed through spectator or annihilation processes. The measurements of $D_s^+ \to \bar{K}^0K^+$ and $D_s^+ \to \bar{K}^{*0}K^+$ relative to $D_s^+ \to \phi\pi^+$ are higher than the theoretical predictions.[25] However, uncertainties in these predictions preclude a definitive statement concerning the relative importance of spectator and non-spectator processes.

We gratefully acknowledge the dedicated efforts of the SPEAR staff. One of us (G.E.) wishes to thank the A. von Humboldt Foundation for support. This work was supported by the Department of Energy, under contracts DE-AC03-76SF00515, DE-AC02-76ER01195, DE-AC03-81ER40050, DE-AC02-87ER40318, DE-AM03-76SF00034 and by the National Science Foundation.

References

1. For a review see M.A. Shifman, in *International Symposium on Lepton and Photon Interactions*, edited by W. Bartel and R. Rückl (North-Holland, Amsterdam, 1987).

2. R.M. Baltrusaitis *et al.*, Phys. Rev. Lett. **56**, 2136 (1986).

3. J. Adler *et al.*, Phys. Rev. Lett. **60**, 1375 (1988).

4. H. Albrecht *et al.*, Phys. Lett. **195B**, 102 (1987).

5. J.C. Anjos *et al.*, Phys. Rev. Lett. **62**, 125 (1989).

6. R.M. Baltrusaitis *et al.*, Phys. Rev. Lett. **54**, 1976 (1984); **55**, 638(E) (1985).

7. J.C. Anjos *et al.*, Phys. Rev. **D37**, 2391 (1988).

8. B. Guberina *et al.*, Phys. Lett. **89B**, 111 (1979); Y. Koide, Phys. Rev. **D20**, 1739 (1979); G. Altarelli and L. Maiani, Phys. Lett. **118B**, 414 (1982).

9. M. Bauer, B. Stech and M. Wirbel, Z. Phys. C **34**, 103 (1987). Revised values of $a_1 = 1.2$ and $a_2 = -0.5$ are taken from B. Stech, preprint HD-THEP-87-18, 1987 (unpublished).

10. We adopt the convention that reference to a state also implies reference to its charge conjugate.

11. D. Bernstein *et al.*, Nucl. Instrum. Methods **226**, 301 (1984).

12. G.T. Blaylock *et al.*, Phys. Rev. Lett. **58**, 2171 (1987).

13. Kaon candidates are required to have a useable TOF measurement t, with $|t - t_K| / \sigma_K < |t - t_\pi| / \sigma_\pi$, where t_π and t_K are the predicted π and K times and σ_π, σ_K are the uncertainties on the time differences. The TOF system provides π-K separation of $> 2\sigma$ over the relevant range of $K^\pm$ momenta ($p < 1.1\,\mathrm{GeV}/c$). All tracks are accepted as pion candidates, except when the measured TOF is inconsistent with the π hypothesis. Further background rejection is obtained from dE/dx measurements for pion candidates not having TOF information.

14. A D_s^* mass of $2.109\,\mathrm{GeV}/c^2$ is used (Reference 12).

15. J. Adler *et al.*, Phys. Lett. **196B**, 107 (1987).

16. R.M. Baltrusaitis *et al.*, Phys. Rev. Lett. **55**, 150 (1985); **56**, 2140 (1986); J. Adler *et al.*, Phys. Rev. Lett. **60**, 89 (1988); Phys. Lett. **208B**, 152 (1988).

17. We use the Jetset 6.2 event generator, T. Sjöstrand, Comput. Phys. Commun. **39**, 347 (1986).

18. The TOF requirement for the the fast pion *not* arising from the K_S^0 decay is made more stringent than that for the other pions. The requirement is analogous to that for the charged kaon in the $D_s^+ \to \bar{K}^0 K^+$ analysis.

19. We use the measurement of $B(D_s^+ \to K^+K^-\pi^+)_{\mathrm{NR}}/B(D_s^+ \to \phi\pi^+)$ from J.C. Anjos *et al.*, Phys. Rev. Lett. **60**, 897 (1988).

20. S. Barlag *et al.*, preprint CERN-EP/88-103, 1988 (unpublished).

21. M.P. Alvarez *et al.*, preprint CERN-EP/88-148, 1988 (unpublished).

22. H. Albrecht *et al.*, Phys. Lett. **179B**, 398 (1986).

23. B.Yu. Blok and M.A. Shifman, Yad. Fiz. **45**, 211 (1987); **45**, 478 (1987); **45**, 841 (1987); **46**, 1310 (1987) [Sov. J. Nucl. Phys. **45**, 135 (1987); **45**, 301 (1987); **45**, 522 (1987); **46**, 767 (1987)].

24. A.N. Kamal and R.C. Verma, Phys. Rev. **D35**, 3515 (1987); **D36**, 3527(E) (1987). The predictions are derived with $\delta^{\pi K} = 100°$. The parameter p in this calculation is constrained by our limit to values < 0.5.

25. Although the Model 1 predictions shown do not include final state interactions, it is interesting to note that better agreement with the data is achieved for the ratios shown in Table I by using $|a_1/a_2| \sim 1.8$.

TABLE I. Relative D_s^+ branching fractions.

	Experiment	Model 1[a]	Model 2[b]	Model 3[c]
$\frac{B(D_s^+ \to \bar{K}^0 K^+)}{B(D_s^+ \to \phi\pi^+)}$	$0.92 \pm 0.32 \pm 0.20$[d]	0.47	0.43	
$\frac{B(D_s^+ \to \bar{K}^{*0} K^+)}{B(D_s^+ \to \phi\pi^+)}$	$0.84 \pm 0.30 \pm 0.22$[d] $0.87 \pm 0.13 \pm 0.05$[e] $0.89 \pm 0.32 \pm 0.13$[f] 0.93 ± 0.37[g] 1.44 ± 0.37[h]	0.55	0.74	
$\frac{B(D_s^+ \to K^0 \pi^+)}{B(D_s^+ \to \bar{K}^0 K^+)}$	< 0.22 (90% CL)[d]	0.20		0.11 to 0.22
$\frac{B(D_s^+ \to K^0 \pi^+)}{B(D_s^+ \to \phi\pi^+)}$	< 0.21 (90% CL)[d]	0.09		

[a]Reference 9.
[b]Reference 23.
[c]Reference 24.
[d]This experiment.
[e]Reference 19.
[f]Reference 20.
[g]Reference 21.
[h]Reference 22.

Figure Captions

1. Inclusive $\pi^+\pi^-$ mass distribution before (unshaded) and after (shaded) the vertex displacement requirement is imposed.

2. (a) $K_S^0 K^+$ mass distribution after kinematic fit. (b) Background distributions predicted by Monte Carlo simulation, normalized to integrated luminosity of the data set. The shaded histogram shows the contribution from $D^*\bar{D}^*$, $D^*\bar{D}$, and $D\bar{D}$ events; the unshaded histogram gives the total for these final states and non-charm continuum events.

3. (a) $K_S^0\pi^+$ mass distribution after kinematic fit. The curve represents the 90% CL upper limit on the number of signal events. (b) Monte Carlo background distributions: D events (shaded) and the sum of D and non-charm continuum events (unshaded).

4. Inclusive $K^-\pi^+$ mass distribution. The enhancements in the high mass region result from $D \to \bar{K}\pi\pi$ and $D \to \bar{K}\pi$.

5. (a) $\bar{K}^{*0}K^+$ mass distribution after kinematic fit, requiring $|\cos\theta_\pi| > 0.3$. (b) Monte Carlo background distributions: D events (shaded) and the sum of D and non-charm continuum events (unshaded).

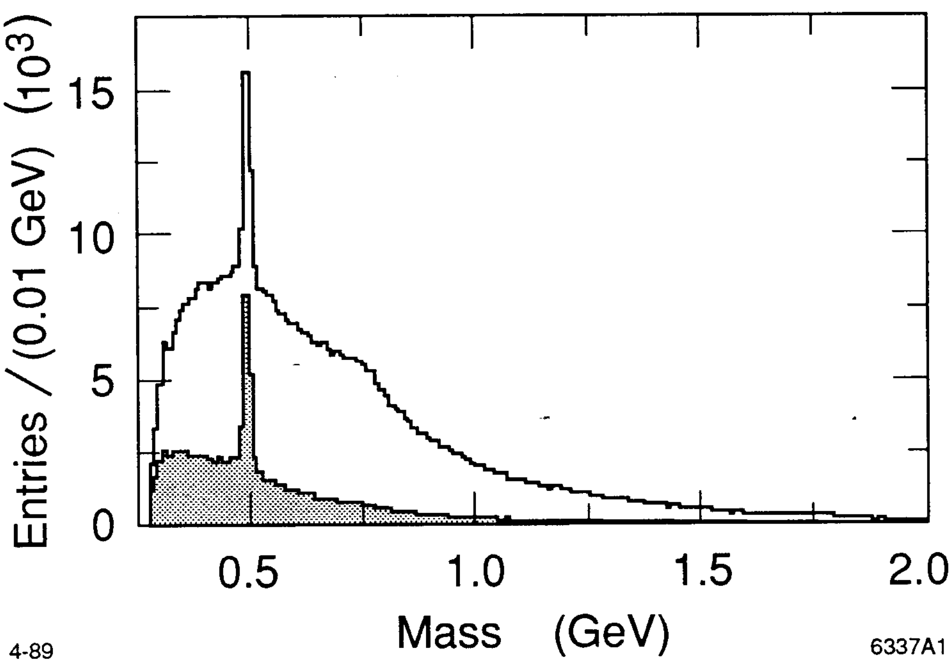

Fig. 1

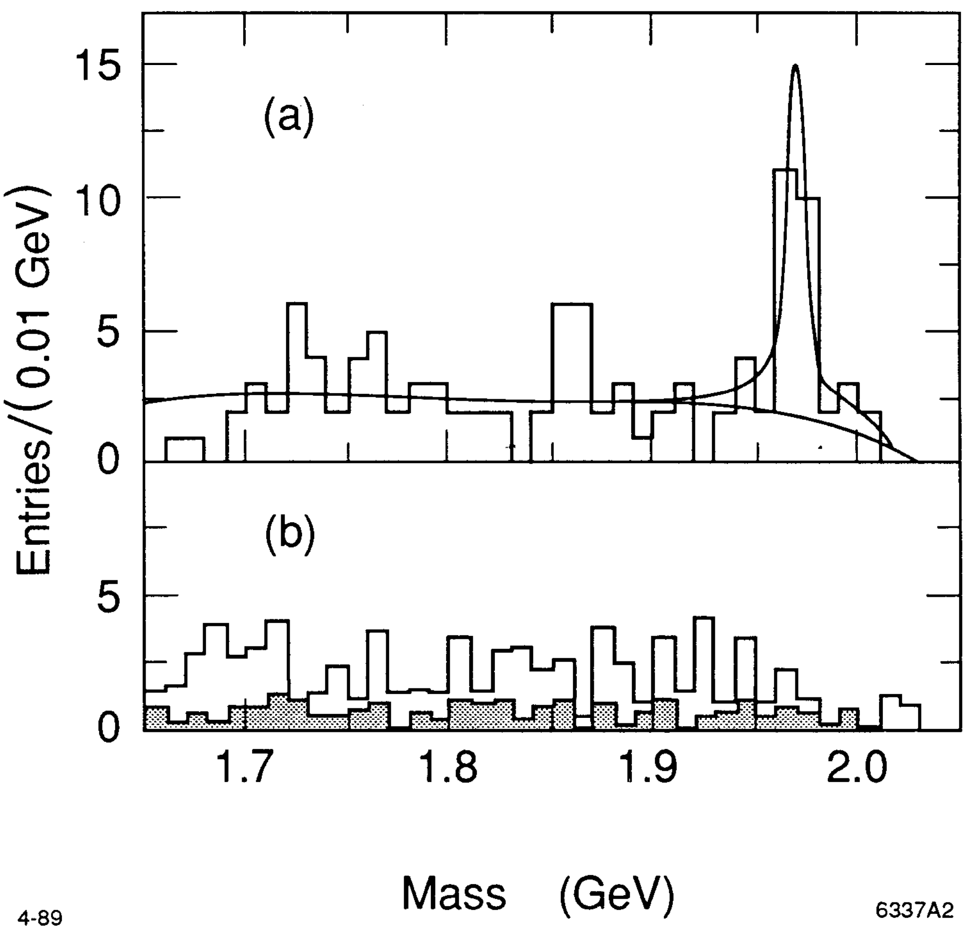

Fig 2

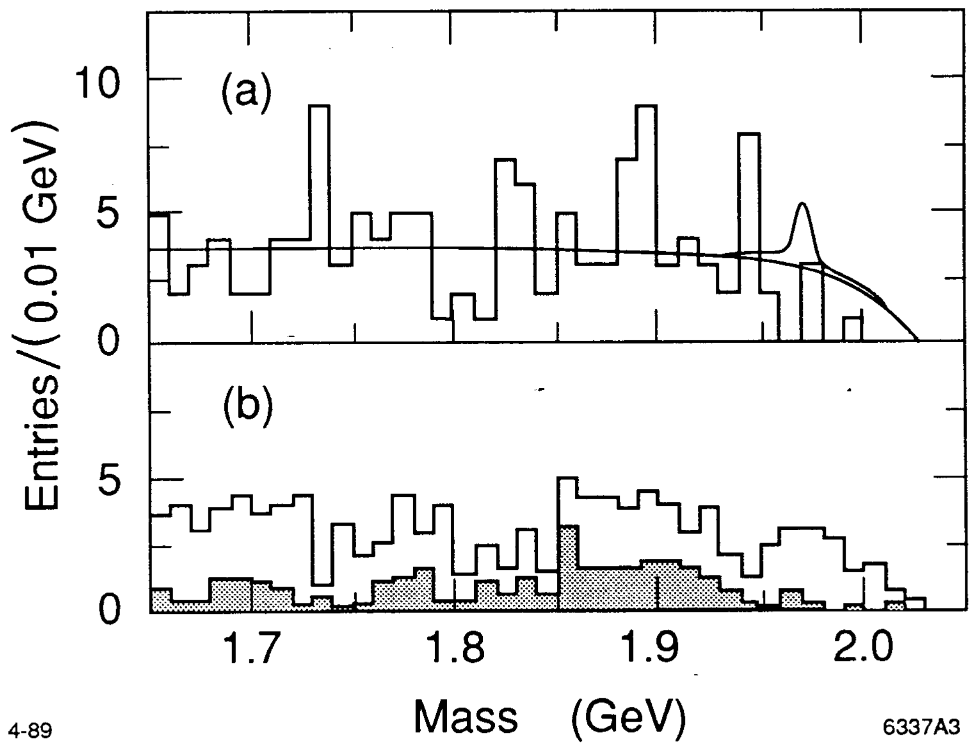

Fig. 3

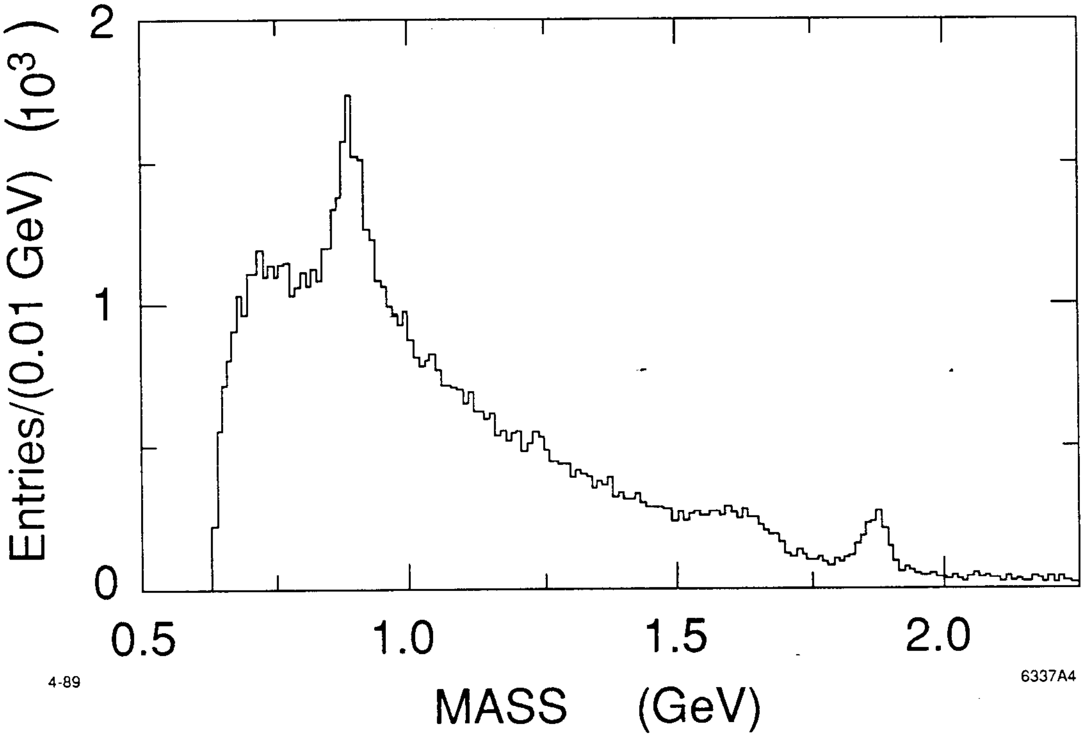

Fig. 4

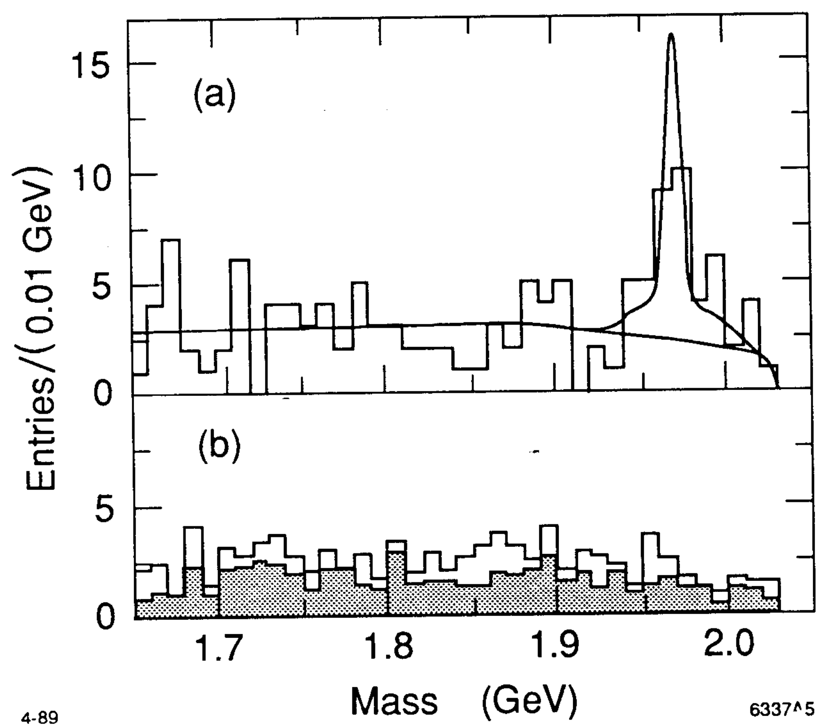

Fig. 5